Structural Correlation between Crystal Lattice and Lamellar Morphology in the Phase Transitions of Uniaxially Oriented Syndiotactic Polystyrene (δ and δ_e Forms) As Revealed by Simultaneous Measurements of Wide-Angle and Small-Angle X-ray Scatterings

E. Bhoje Gowd, Naoya Shibayama, and Kohji Tashiro*

Department of Future Industry-oriented Basic Science and Materials, Graduate School of Engineering, Toyota Technological Institute, Tempaku, Nagoya 468-8511, Japan

Received August 6, 2007; Revised Manuscript Received January 17, 2008

ABSTRACT: The simultaneous measurement of wide-angle (WAXS) and small-angle X-ray scattering (SAXS) patterns has been made successfully for the first time for the uniaxially oriented δ (filled clathrate) and δ_e (emptied clathrate) forms during the heating process. The basic idea behind these measurements is to clarify the correlation between the crystal structure change and the morphological change of the stacked lamella. At room temperature the δ and δ_e forms showed a two-point scattering pattern, indicating the stacked lamellar structure. However, in the δ_e form the two-point scattering pattern was completely masked by strong diffused scattering because of the empty cavities in the crystal lattice due to the removal of solvent molecules. WAXS and SAXS results revealed that the δ to γ phase transition occurs smoothly without disturbing the stacked lamellar structure very much. On the other hand, a major reorganization in the stacked lamellar structure was observed in the case of δ_e to γ transition through a disordered structure (intermediate form). These results suggest that the solvent molecules, which are residing in the crystal lattice, play a crucial role in the phase transition from δ to γ form. At higher temperatures around 190–200 °C, the γ form was found to transform to the α (and partially β) form. The long period and lamellar thickness increased remarkably during this γ to α (β) transition. It is shown that the large change in the stacked lamellae during this γ to α (β) transition is not only due to the unraveling of the helices into planar-zigzag form but also because of the number of repeating units at the boundary of crystalline and amorphous region increases.

Introduction

The application of external condition, e.g., temperature, solvent atmosphere, etc., causes quite complicated phase transitions in syndiotactic polystyrene (sPS). This complex polymorphic behavior has been extensively studied for the past two decades.[1–30] Among the four crystalline forms (α, β, γ, and δ) of sPS, the α and β forms take all-trans planar-zigzag (T_4) conformation while the γ and δ forms take helical conformation [-(T_2G_2)$_2$-].[1–7] Besides these four crystalline forms, a mesophase of all-trans planar-zigzag conformation was also reported, which can be obtained by stretching the amorphous sample around the glass transition temperature.[8] Of these various crystalline forms of sPS, the δ form is unique in such a point that the sPS polymer and the solvent molecules form the clathrate in the crystalline region.[9–13] Moreover, by extracting the solvent molecules from the δ form in acetone and further rinsing in methanol or by extracting the δ form in supercritical CO_2, the so-called empty δ (δ_e) form can be obtained.[14–18] The δ_e form retains the helical structure similar to the δ and γ forms but with the cavities which had been occupied by solvent molecules.[14–18] These cavities are of angstrom size and are considered to be useful for the separation of solvent molecules of a particular size from the mixture of solvents. Because of this characteristic behavior, the δ_e form has been proposed as a molecular filter for the purification of water and air and also in the field of chemical separation engineering.[19,20] More recently, films of sPS in the δ_e form have been proposed as the material for molecular sensors.[21,22] From such an industrial application it is also important to understand the structural changes of the δ and δ_e forms during heating.

Structural changes in thermally induced phase transitions of the δ form have been investigated well using various techniques including X-ray and electron diffraction,[4,6,15,18,23,24] infrared and Raman spectroscopy,[25–31] solid-state NMR,[32,33] and conformational energy analysis.[34,35] It has been found that the δ form transforms to the γ form above 100 °C without passing through the δ_e form or intermediate form.[23,25,28,29] The transition from δ to γ form depends on the relative amount of solvent present in the system.[23] Unlike the δ form, the δ_e form behaves differently because of the cavities present in the crystal lattice. When the δ_e form is heated, it transforms to an intermediate form before transforming into the γ form.[15,18,24] The intermediate form detected during the δ_e to γ transition was shown to take the structure of disordered chain packing.[18] It has been reported that the γ form transforms to the α form at higher temperature around 180–190 °C.[3,15,23,25] More recently, we showed that the γ form transformed to the mixture of α and β forms rather than into the pure α form in uniaxially oriented samples and bulk samples with relatively large thickness.[36,37] The solvent molecules, transiently residing in the amorphous region on the way of transition from δ to γ (because of the slow diffusion in bulky and oriented samples), are responsible for the appearance of the β form along with the α form.[36,37] Though the phase transitions have been known in this way, the details of the structural changes and the relationship between the chain-packing mode in the crystal lattice and the stacked structure of crystalline lamellae has not yet been clarified well enough. Moyses et al.[38,39] grew the crystals of the sPS/ethylbenzene complex from dilute solutions and reported the long period changes during the δ to γ transition. They attributed these changes to decomplexation of solvent molecules and promotion of lamellar thickening in the presence of solvent

* To whom correspondence should be addressed.

10.1021/ma071759z CCC: $40.75
Published on Web 02/28/2008

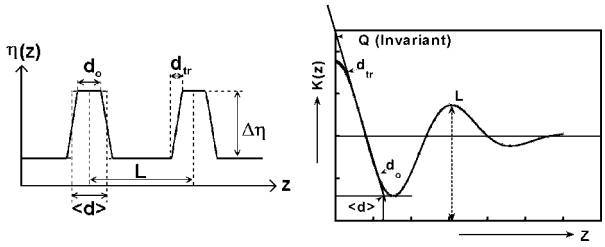

Figure 1. Electron density distribution $\eta(z)$ and the one-dimensional electron density correlation function $K(z)$ for the lamellar system. Q is the invariant, d_{tr} the thickness of the transition zone between the crystalline lamella and amorphous part, d_0 the thickness of the lamellar core, $\langle d \rangle$ the mean lamellar thickness, and L the long period.

molecules. In their studies, the X-ray diffraction profiles were measured at room temperature after annealing the samples at higher temperatures. To clarify the phase transition behavior of the δ and δ_e forms more clearly, we need to carry out the simultaneous measurements of WAXS/SAXS during the heating process.

We could successfully measure the temperature dependence of the X-ray fiber diagrams of WAXS/SAXS simultaneously starting from the uniaxially oriented δ and δ_e forms using a single imaging plate detector by adjusting the sample-to-camera distance to a suitable value. The reason why the uniaxially oriented samples were used here is that the transition behavior can be clarified much better by separating the equatorial and layer line reflections. To our knowledge, no article appeared on the SAXS measurements of the δ_e form even at room temperature. Besides, for the first time we measured the temperature dependence of the SAXS patterns simultaneously with the WAXS patterns of the δ and δ_e forms in the heating process and compared the phase transition behavior. We believe that the present data should make a significant contribution to better understanding of the essential features of the δ and δ_e forms and also phase transitions of sPS.

Experimental Section

Samples. sPS pellets (M_w = 272 000, M_w/M_n = 2.28) were kindly supplied by Idemitsu Petrochemical Co., Ltd. The glassy samples were prepared by quenching the melt into ice–water. A small piece of rectangular shape was cut out of the amorphous strip and stretched by about 5 times the original length above the hot plate around the glass transition temperature (97 °C). These uniaxially oriented samples were dipped in different solvents like toluene and chloroform for 2 days at ambient temperature to obtain the δ form, where almost no shrinkage occurred about the sample length. It should be noticed here that the uniaxial drawing of the glassy sample results in the formation of the disordered aggregation state of essentially planar-zigzag chains and transforms to the oriented δ form by supplying the solvent molecule. The samples removed from the solvents were kept at ambient temperature until they became perfectly dry. The δ_e form was obtained by refluxing the δ form samples in acetone for 15 h followed by being refluxed in methanol for 8 h to remove the residual acetone. The absence of solvent molecules in the δ_e form was confirmed by thermogravimetric analysis (TGA) measurements.

Measurements. WAXS and SAXS patterns of the uniaxially oriented samples were measured by using a MAC Science DIP 1000 imaging plate system with an X-ray generator of a rotating anode type. The graphite-monochromatized Cu Kα line was used as an incident X-ray beam. In order to take the two-dimensional WAXS and SAXS patterns simultaneously on a sheet of imaging plate of 20 cm diameter, the sample-to-imaging plate distance was set to 260 mm. The collimator of 0.3 mm diameter was used, and the homemade small beam stopper was set above the imaging plate to detect the SAXS pattern. The uniaxially oriented sample was set into a homemade heater block, and the temperature of the sample

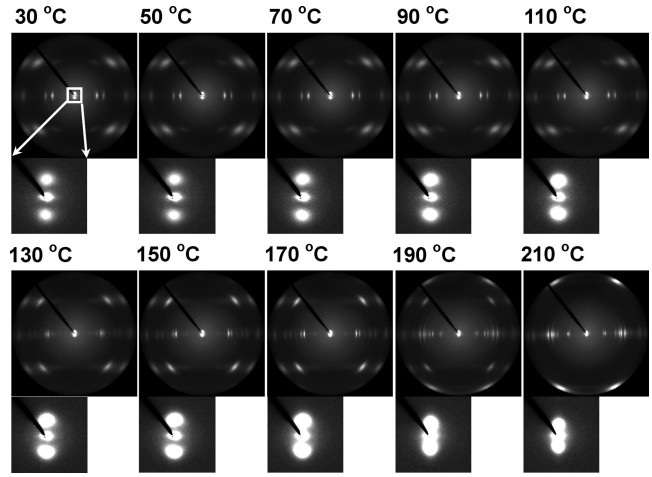

Figure 2. Temperature dependence of the WAXS and SAXS patterns measured simultaneously using a single imaging plate for the uniaxially oriented δ form of the sPS/toluene complex in the heating process. SAXS patterns are expanded and showed below the respective WAXS pattern for the purpose of clarity. The draw axis is along the vertical direction. The SAXS patterns are enlarged as shown below the fiber diagrams.

was monitored using a thermocouple contacted directly to the sample. WAXS and SAXS patterns were recorded during the heating process.

SAXS Data Analysis. The two-dimensional SAXS intensity was first integrated to obtain the scattering pattern as a function of $q = (4\pi \sin \theta)/\lambda$, 2θ being the scattering angle and λ the X-ray wavelength. To examine the lamellar structures, the one-dimensional electron-density correlation function $K(z)$ was calculated from the SAXS data. Under the assumption of the two-phase model consisting of the alternately stacked structure of the crystalline and amorphous layers, the $K(z)$ is defined as follows.[40,41]

$$K(Z) = \langle [\eta(Z') - \langle \eta \rangle][\{\eta(Z+Z') - \langle \eta \rangle\}] \rangle \propto \int_0^\infty l(q) q^2 \cos qz \, dq \quad (1)$$

where $\langle\ \rangle$ is the statistical average and $\eta(z)$ and $\langle \eta \rangle$ are the electron density variation along the lamellar normal on the z axis and the mean electron density, respectively. Various points indicated on the $K(z)$ curve give various physical parameters as shown in Figure 1: the invariant Q, the mean lamellar thickness $\langle d \rangle$, the mean boundary thickness d_{tr}, the mean core thickness d_0, and the long period L.[40,41]

Results and Discussion

Lamellar Morphology Change during the δ to γ Transition. WAXS and SAXS patterns were measured simultaneously for the uniaxially oriented δ form of the sPS−toluene complex in the heating process. The two-dimensional WAXS and SAXS image series are shown in Figure 2 at different temperatures starting from the uniaxially oriented δ form. The change in the equatorial (WAXS) and the meridional (SAXS) profiles evaluated from the two-dimensional fiber diagram in the heating process are shown in parts a and b of Figure 3, respectively. The temperature dependence of the integrated intensities of various reflections corresponding to each crystalline form (δ, γ, α, and β) is shown in Figure 4. WAXS results revealed that the phase transition from δ to γ occurs over a broad range of temperature 100–130 °C, and both the δ and γ forms coexist in this temperature range. The corresponding SAXS patterns did not show any obvious change in this temperature range as seen in Figures 2 and 3b other than a small shift of the scattering peak position. In order to understand the intimate correlation between the crystal structure change and

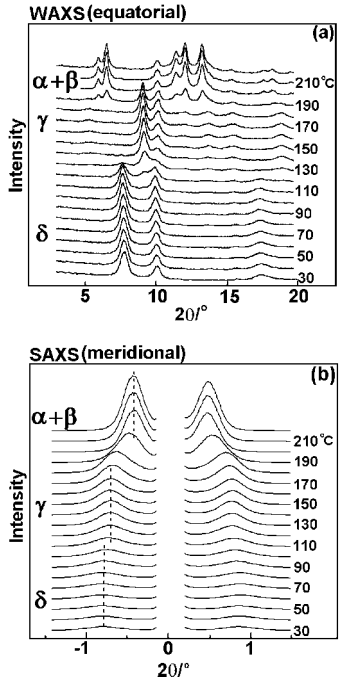

Figure 3. Temperature dependence of X-ray diffraction profile on the (a) equatorial line (WAXS) and (b) meridional line (SAXS) extracted from Figure 2.

the stacked lamellar structural change, we analyzed the SAXS results by calculating one-dimensional electron density correlation functions and compared them with the WAXS results. The one-dimensional electron density correlation function ($K(z)$) curves at various temperatures in the heating process are shown in Figure 5. The long period (L), lamellar thickness ($\langle d \rangle$), and invariant (Q) were estimated from $K(z)$ curves and are plotted as a function of temperature as shown in Figure 4. A slight increase in the lamellar thickness and long period was observed during the δ to γ transition by retaining the stacked lamellar structure. Moyses et al.[38,39] also observed an increase in long period during the δ to γ transition and related such an increase to lamellar thickening in the presence of solvent molecules. Also, they proposed an intermediate structure with disordered chain segments during the δ to γ transition.[38] However, as shown in Figures 2 and 3, the WAXS patterns do not suggest any generation of such a disordered structure in the temperature region of the δ to γ transition. The invariant (Q) estimated from the one-dimensional electron density correlation function curves (see Figure 1) are plotted against temperature as shown in Figure 4. The change in Q reflects the change in the electron density gap between the crystalline and amorphous regions. On the basis of these Q values, we estimated roughly the change in the electron density gap between the crystalline ($\eta_{e,c}$) and amorphous ($\eta_{e,a}$) regions ($\Delta\eta$) using the following equation.[40]

$$\Delta\eta = \eta_{ec} - \eta_{ea} = (Q/\varphi_c(1-\varphi_c))^{1/2} \quad (2)$$

where φ_c is the crystallinity estimated from the lamellar thickness $\langle d \rangle$ and the long period (L):

$$\varphi_c = \langle d \rangle / L \quad (3)$$

On heating, the Q and $\Delta\eta$ values increased slowly because of the difference in the thermal expansion coefficients between the amorphous and crystalline phases. The evaporation of toluene molecules during the δ to γ transition may also contribute to some extent for such an increase in the Q and $\Delta\eta$ values on heating. Above all, the change in the density fluctuation between the crystalline and amorphous phases strongly influences the

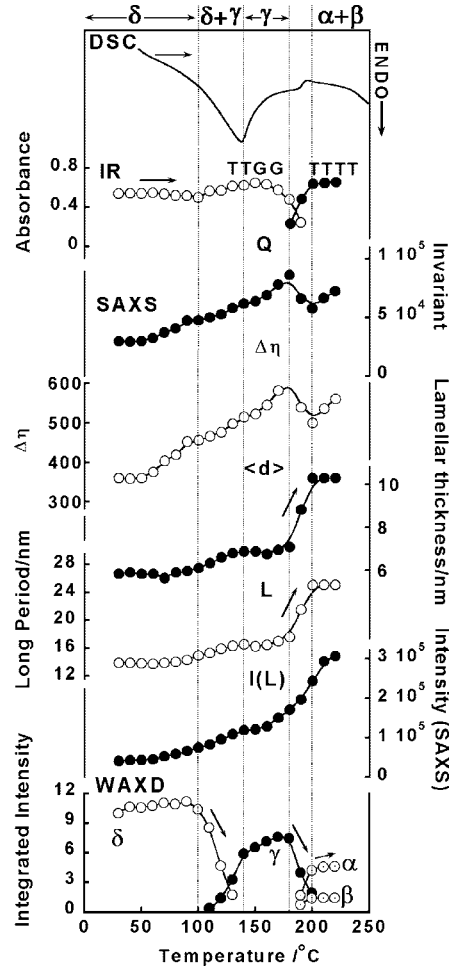

Figure 4. Temperature dependence of the various parameters obtained by the calculations of the correlation functions from the SAXS profiles and integrated intensities of the reflections at $2\theta = 8.0°$ (δ), 9.1° (γ), 6.5° (α), and 6.0° (β) evaluated from Figure 3a of the uniaxially oriented δ form of sPS/toluene complex in the heating process. The infrared spectral data and DSC thermogram of the uniaxially oriented δ form in the heating process are also shown for the purpose of comparison.

SAXS intensity, and the SAXS intensity $I(L)$ also increased during the δ to γ transition as seen in Figure 4.

To know the more concrete structural change in the phase transition process, the WAXS and SAXS results are compared also with the infrared spectral data and DSC thermogram in Figure 4, which were reported in our previous article.[36] The broad endotherm in DSC thermogram and the disappearance of the solvent band in infrared spectra confirmed the solvent evaporation process during the δ to γ transition. The phase transition from the δ to γ form occurs in a broad temperature range, and the helical (T_2G_2) content remains the same during this process. At the same temperature the 2-D WAXS patterns may be assumed as a simple overlap of the two types of diagrams due to the coexistence of δ and γ forms, and the corresponding SAXS patterns also retain the stacked lamellar structure. Different from the case of the δ_e to γ transition to be mentioned in the next section, there appears no intermediate phase on the δ to γ transition. Therefore, we may say that the solvent molecules in the crystal lattice of the δ form might help the δ to γ transition to occur smoothly without disturbing the stacked lamellar structure. Once the solvent molecules leave the crystal lattice, the structure becomes unstable and transforms immediately to the γ form without any passage to the intermediate form or δ_e form. At higher temperature, the γ form transforms into the mixture of α and β forms in a narrow

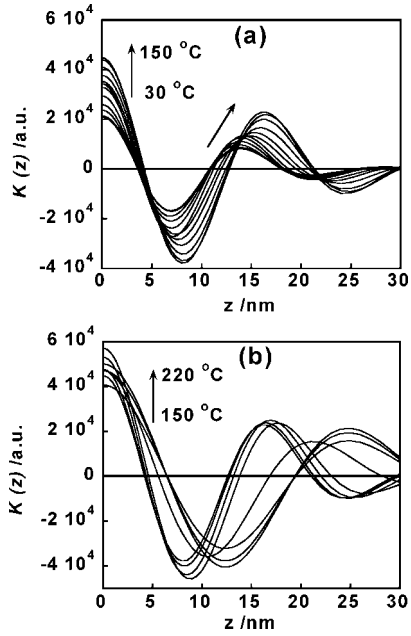

Figure 5. One-dimensional electron density correlation function $K(z)$ estimated from the SAXS pattern for the uniaxially oriented δ form of the sPS/toluene complex in the heating process (a) 30–150 °C and (b) 150–220 °C.

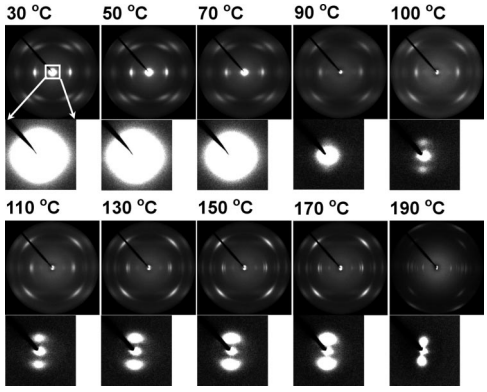

Figure 6. Temperature dependence of the WAXS and SAXS patterns measured simultaneously using a single imaging plate for the uniaxially oriented δ_e form of the sPS/chloroform complex in the heating process. SAXS patterns are expanded and showed below the respective WAXS pattern for the purpose of clarity. The draw axis is along the vertical direction. The SAXS patterns are enlarged and shown below the fiber diagrams.

temperature range of 180–190 °C, and the transition will be discussed in a later section.

Lamellar Morphology Change during the δ_e to γ Transition. In the previous section we have seen the transition behavior of the δ form where the solvent molecules are residing in the crystal lattice. These solvent molecules were extracted from the crystal lattice of the δ form using suitable procedures as described in the Experimental Section. This section follows the structural change in the uniaxially oriented δ_e form of the sPS/chloroform complex. Figure 6 shows the WAXS and SAXS patterns at different temperatures starting from the uniaxially oriented δ_e form of sPS/chloroform complex in the heating process. The room temperature SAXS pattern shows a strong diffuse scattering, which may come from the electron density contrast between the empty cavities and the actual entities in the δ_e form. Such diffuse scattering is not observed in the case of δ form (Figure 2), where the cavities are filled with the

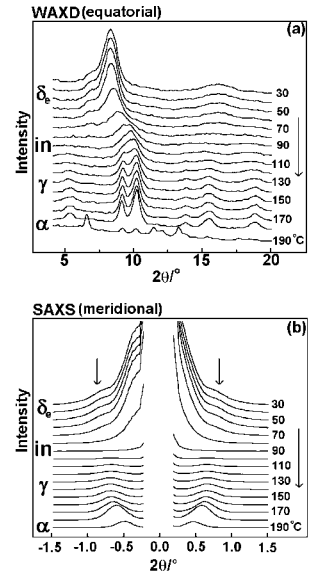

Figure 7. Temperature dependence of X-ray diffraction profile on the (a) equatorial line (WAXS) and (b) meridional line (SAXS) extracted from Figure 6.

solvent molecules. The one-dimensional profile scanned along the meriodional line shows a typical two-point scattering pattern at room temperature along with the strong diffuse scattering. The change in the equatorial (WAXS) and the meridional (SAXS) patterns evaluated from the two-dimensional fiber diagram in the heating process are shown in parts a and b of Figure 7, respectively. The temperature dependence of the integrated intensities of various reflections corresponding to each crystalline form is given in Figure 8. As the temperature was increased, a new WAXS pattern was observed in the temperature range 70–100 °C, which was different from those of the δ_e and γ forms. Manfredi et al.[15] called this form as a helical mesophase. As we have not yet known the detailed packing structure of this form, we called this phase as an "intermediate phase" in our previous paper.[18]

When we look at the corresponding SAXS patterns, drastic changes were observed in the SAXS intensity as well as the position of the scattering peak with the increase in temperature. As seen in Figures 6 and 7b, the diffuse scattering, which was strong at room temperature, started decreasing in intensity from 70 °C and almost disappeared at 100 °C. As pointed out above, the diffuse scattering appeared in the δ_e form because of the empty cavities present in the crysta,l lattice. The decrease and disappearance of the diffuse scattering in SAXS patterns suggest that these cavities started to be erased from the crystal lattice at 70 °C, and almost all the cavities disappeared perfectly at 100 °C during heating. These results suggest a strong relationship between the disappearance of the empty cavities from the crystal lattice of the δ_e form and the appearance of the intermediate form in this temperature range.

Figure 9 shows the calculated one-dimensional electron density correlation function curves at various temperatures during heating. Thus, estimated long period (L), lamellar thickness ($\langle d \rangle$) , and invariant (Q) are plotted as a function of temperature as shown in Figure 8. L and $\langle d \rangle$ values remain unchanged up to 60 °C and then drastically increased in the temperature range 70–120 °C, suggesting that the lamellae undergo reorganization in this temperature range. In the same temperature range the WAXS data showed that the crystalline phase undergoes a dramatic change from δ_e to intermediate form. The large changes in the crystalline phase affect the organization at the lamellar level. Above 120 °C, both L and

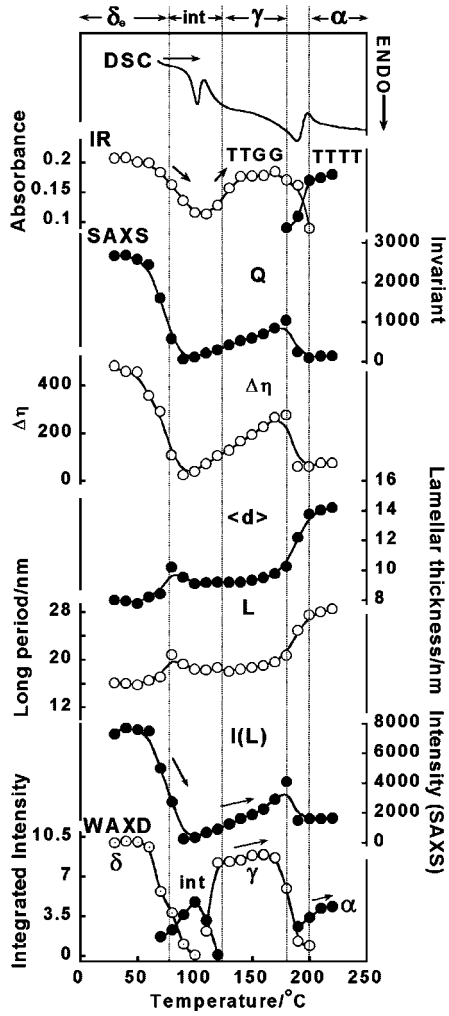

Figure 8. Temperature dependence of the various parameters obtained by the calculations of the correlation functions from the SAXS profiles and integrated intensities of the reflections (WAXS) at $2\theta = 8.0°$ (δ_e), 9.6° (intermediate), and 9.1° (γ) evaluated from Figure 7a of uniaxially oriented δ_e form of the sPS/chloroform complex in the heating process. The infrared spectral data and DSC thermogram of the uniaxially oriented δ_e form in the heating process are also shown for the purpose of comparison.

$\langle d \rangle$ remain unchanged up to 180 °C. The Q and $\Delta\eta$ values changed drastically during the transitions from the δ_e form to the intermediate phase and to the γ form, which is entirely different from the case of δ to γ transition as seen in the previous section.

The information obtained by WAXS/SAXS data is compared with that obtained by infrared spectral and DSC data (taken from the previous paper for the purpose of comparison[18]), as shown in Figure 8. In our previous paper, we speculated that the intermediate form takes a disordered structure affected by the empty cavities present in the crystal lattice.[18] In the δ_e form, the helical chains (T_2G_2) are packed in the crystal lattice with many cavities as known from a strong diffuse scattering of the SAXS pattern. On heating the diffuse scattering of the SAXS pattern started decreasing in the temperature range 70–100 °C, indicating the disappearance of the empty cavities. In parallel, the infrared spectral data showed a decrease in the T_2G_2 content. Therefore, we may say that the disappearance of the empty cavities causes the transient decrease of regular helical segments, resulting in the formation of the structurally disordered intermediate phase. On further heating, the conformationally disordered chains are rearranged to form the regular γ form crystal as known from the increment of infrared T_2G_2 band intensity. Increase in $\Delta\eta$ and Q is related with this structural ordering process.

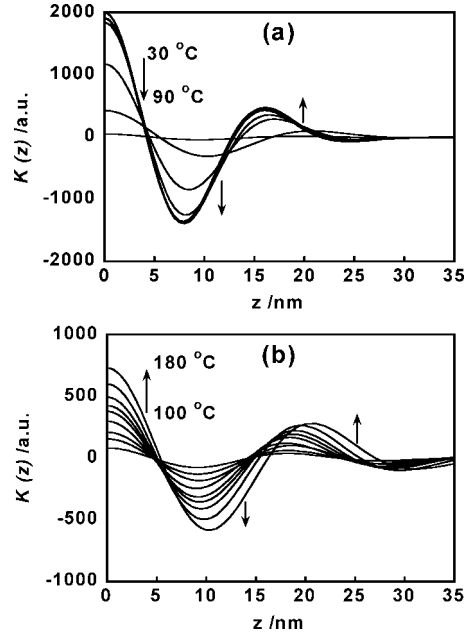

Figure 9. One-dimensional electron density correlation function $K(z)$ estimated from the SAXS pattern for the uniaxially oriented δ_e form of sPS/chloroform complex in the heating process at an interval of every 10 °C: (a) 30–90 °C and (b) 100–180 °C.

Lamellar Morphology Change during the γ to α (β) Transition. As seen in the previous sections, the γ form transferred into the α (β) forms at higher temperature. But the relative content of the β form is different depending on the starting sample, i.e., δ or δ_e form. The δ form sample showed higher content of the β form at higher temperatures, whereas the δ_e form showed only the α form. These results are in good agreement with the recently published paper,[37] where we showed that the solvent molecules, which are excluded from the crystal lattice of the δ form, are responsible for the appearance of the β form.

The two-dimensional X-ray fiber diagrams (Figures 2 and 6) in the temperature region 180–190 °C can be assumed as a simple overlap of the γ and α (β) forms. These fiber patterns do not indicate any disordering and ordering of the chains in the crystal. The corresponding SAXS patterns were analyzed, and the long period and lamellar thickness increased remarkably during the γ to α (β) transition, as seen in Figure 4. These results indicate a major structural reorganization process in the stacked lamellar structure during the transition process. The phase transition between the γ and α (β) forms involves the unraveling of helical (T_2G_2) chains into planar-zigzag chains (all-trans), i.e., the conformational change. It is important to highlight that the conformational change affects not only the inner structure of the crystallite but also the lamellar stacking structure of the whole sample. On the basis of such observations that the molecular chains kept the orientation almost perfectly as known from the X-ray diffraction patterns and that the lamellar stacking structure was also kept, the endotherm in the DSC thermogram might correspond to the process of conformational transformation during the phase transition from T_2G_2 to $(T_2)_2$ forms. The lamellar thickness at high temperature becomes rather larger because of the violent translational motion of chains along the chain axis, which might be caused by an exchange between TG and TT conformations. During this process, the number of repeating units at the boundary of crystalline and amorphous

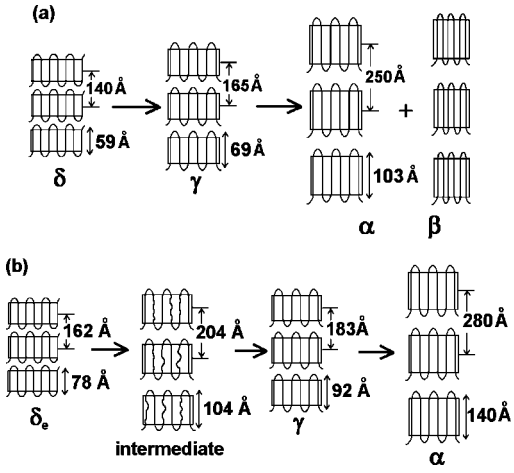

Figure 10. Illustrated stacked lamellar structure in the heating process of the (a) δ form and (b) δ_e form.

region increases. This large morphological change is detected as an exothermic peak of DSC thermogram, indicating an energetic stabilization of lamellar stacking structure. Such an intimate relation between the conformational transformation in the crystallites and the change in stacked lamellar structure was proposed for the phase transition from high-temperature phase to low-temperature phase of vinylidene fluoride−trifluoroethylene copolymers in the heating process.[42]

Figure 10 shows the schematic illustration of the phase transition behaviors of sPS starting from the δ and δ_e forms. The stacked lamellar structure was kept almost perfect during the δ to γ transition due to the solvent molecules present in the crystal lattice of the starting δ form, whereas major reorganization in the stacked lamellar structure was observed during the δ_e to γ transition due to the empty cavities in the δ_e form. At higher temperature, the γ form transformed to the α and β forms depending on the starting sample as mentioned in the earlier sections. The large change in the stacked lamellar structure occurs in association with the unraveling of the helices into planar-zigzag form and the disordering at the boundary of crystalline and amorphous region, during which the chain orientation is kept almost perfect. It is important to point out that the structural changes in the crystalline region are intimately related with the changes in the lamellar stacking mode during δ to γ, δ_e to γ, and γ to α (β) transitions.

Conclusions

In the present paper we measured the two-dimensional WAXS and SAXS patterns simultaneously in the heating process of the uniaxially oriented δ and δ_e forms of sPS. The WAXS and SAXS patterns were found to change remarkably, and the quantitative analysis revealed an intimate relationship of the complicated changes between the crystalline structure and the stacked lamellar structure. When the solvent molecules are extracted from the crystal lattice of the δ form (δ_e form), the strong SAXS diffuse scattering is detected at room temperature because of the empty cavities in the crystal lattice. On heating the δ form transforms to the γ form in a broad temperature region from 100 to 130 °C without disturbing the stacked lamellar structure due to the solvent molecules present in the crystal lattice of the starting δ form. On the other hand, the δ_e form transforms to the intermediate form transiently before transforming into the γ form in a temperature region 80–110 °C. The decrease in the strong diffuse scattering in SAXS pattern and also change in different parameters like long period, lamellar thickness, and invariant suggested that the empty cavities in the crystal lattice of the δ_e form are responsible for the appearance of the intermediate form. As the temperature increased furthermore, the γ form transformed to the α and β forms in the temperature region 180–200 °C. SAXS data revealed that major changes in the stacked lamellar structure occurred during this γ to α (β) transition by keeping the chain orientation perfect. The activated thermal motion of molecular chains occurs at high temperature, causing a remarkable change in molecular conformation, the chain-packing mode in the crystal lattice, and the remarkable increase in the lamellar thickness as well as the long period.

Acknowledgment. This work was financially supported by MEXT "Collaboration with Local Communities" Project (2005–2009). The authors thank Idemitsu Petrochemicals Co. Ltd., Japan, for supplying the sPS sample.

References and Notes

(1) Kobayashi, M.; Nakaoki, T.; Ishihara, N. *Macromolecules* **1989**, *22*, 4377–4382.
(2) Vittoria, V.; Filho, A. R.; De Candia, F. *J. Macromol. Sci., Phys.* **1990**, *B29*, 411–428.
(3) Guerra, G.; Vitagliano, V. M.; De Rosa, C.; Petraccone, V.; Corradini, P. *Macromolecules* **1990**, *23*, 1539–1544.
(4) Greis, O.; Xu, Y.; Arsano, T.; Petermann, J. *Polymer* **1989**, *30*, 590–594.
(5) Immirzi, A.; De Candia, F.; Iannelli, P.; Zambelli, A.; Vittoria, V. *Makromol. Chem., Rapid Commun.* **1988**, *9*, 761–764.
(6) Vittoria, V.; De Candia, F.; Iannelli, P.; Immirzi, A. *Makromol. Chem., Rapid Commun.* **1988**, *9*, 765–769.
(7) Reynolds, N. M.; Savage, J. D.; Hsu, S. L. *Macromolecules* **1989**, *22*, 2867–2869.
(8) Auriemma, F.; Petraccone, V.; Poggetto, F. D.; De Rosa, C.; Guerra, G.; Manfredi, C.; Corradini, P. *Macromolecules* **1993**, *26*, 3772–3777.
(9) Chatani, Y.; Shimane, Y.; Inagaki, T.; Ijitsu, T.; Yukinari, T.; Shikuma, H. *Polymer* **1993**, *34*, 1620–1624.
(10) Chatani, Y.; Inagaki, T.; Shimane, Y.; Shikuma, H. *Polymer* **1993**, *34*, 4841–4845.
(11) De Rosa, C.; Rizzo, P.; Ruiz de Ballesteros, O.; Petraccone, V.; Guerra, G. *Polymer* **1999**, *40*, 2103–2128.
(12) Tarallo, O.; Petraccone, V. *Macromol. Chem. Phys.* **2005**, *206*, 672–679.
(13) Stegmaier, P.; De Girolamo Del Mauro, A.; Venditto, V.; Guerra, G. *Adv. Mater.* **2005**, *17*, 1166–1168.
(14) Reverchon, E.; Guerra, G.; Venditto, V. *J. Appl. Polym. Sci.* **1999**, *74*, 2077–2082.
(15) Manfredi, C.; De Rosa, C.; Guerra, G.; Rapacciuolo, M.; Auriemma, F.; Corradini, P. *Macromol. Chem. Phys.* **1995**, *196*, 2795–2808.
(16) De Rosa, C.; Guerra, G.; Petraccone, V.; Pirozzi, B. *Macromolecules* **1997**, *30*, 4147–4152.
(17) Ma, W.; Yu, J.; He, J. *Macromolecules* **2005**, *38*, 4755–4760.
(18) Gowd, E. B.; Shibayama, N.; Tashiro, K. *Macromolecules* **2006**, *39*, 8412–8416.
(19) Guerra, G.; Milano, G.; Venditto, V.; Musto, P.; De Rosa, C.; Cavallo, L. *Chem. Mater.* **2000**, *12*, 363–368.
(20) Milano, G.; Venditto, V.; Guerra, G.; Cavallo, L.; Ciambelli, P.; Sannino, D. *Chem. Mater.* **2001**, *13*, 1506–1511.
(21) Mensitieri, G.; Venditto, V.; Guerra, G. *Sens. Actuators, B* **2003**, *92*, 255–261.
(22) Giordano, M.; Russo, M.; Cusano, A.; Mensitieri, G.; Guerra, G. *Sensors Actuators, B* **2005**, *109*, 177–184.
(23) Gowd, E. B.; Nair, S. S.; Ramesh, C. *Macromolecules* **2002**, *35*, 8509–8514.
(24) Gowd, E. B.; Shibayama, N.; Tashiro, K. *Macromol. Symp.* **2006**, *241*, 257–261.
(25) Gowd, E. B.; Nair, S. S.; Ramesh, C.; Tashiro, K. *Macromolecules* **2003**, *36*, 7388–7397.
(26) Reynolds, N. M.; Hsu, S. L. *Macromolecules* **1990**, *23*, 3463–3472.
(27) Kobayashi, M.; Nakaoki, T.; Ishihara, N. *Macromolecules* **1990**, *23*, 78–83.
(28) Yoshioka, A.; Tashiro, K. *Macromolecules* **2003**, *36*, 3593–3600.
(29) Yoshioka, A.; Tashiro, K. *Macromolecules* **2003**, *36*, 3001–3003.
(30) Reynolds, N. M.; Stidham, H. D.; Hsu, S. L. *Macromolecules* **1991**, *24*, 3662–3665.
(31) Kellar, E. J. C.; Galiotis, C.; Andrews, E. H. *Macromolecules* **1996**, *29*, 3515–3520.
(32) Capitani, D.; De Rosa, C.; Ferrando, A.; Grassi, A.; Segre, A. L. *Macromolecules* **1992**, *25*, 3874–3880.

(33) Gomezls, M. A.; Tonelli, A. E. *Macromolecules* **1990**, *23*, 3385–3386.
(34) Tamai, Y.; Fukuda, M. *Macromol. Rapid Commun.* **2002**, *23*, 891–895.
(35) Tamai, Y.; Fukuda, M. *J. Chem. Phys.* **2004**, *121*, 12085–12093.
(36) Gowd, E. B.; Shibayama, N.; Tashiro, K. *Macromolecules*, in press.
(37) Gowd, E. B.; Tashiro, K. *Macromolecules* **2007**, *40*, 5366–5371.
(38) Moyses, S.; Sonntag, P.; Spells, S. J.; Laveix, O. *Polymer* **1998**, *39*, 3537–3544.
(39) Moyses, S.; Sonntag, P.; Spells, S. J. *Macromol. Symp.* **1997**, *114*, 145–150.
(40) Strobl, G. R.; Schneider, M. *J. Polym Sci., Polym. Phys. Ed.* **1980**, *18*, 1343–1359.
(41) Strobl, G. R. *Phys. Polym.* **1997**, 408–414.
(42) Tashiro, K.; Tanaka, R. *Polymer* **2006**, *47*, 5433–5444.

MA071759Z